

Cognitive Explainers of Graph Neural Networks Based on Medical Concepts

Yingni Wang, Huabin Zhang*, Lichong Dong, Xiaobo Zhou, and Kehong Yuan*

Abstract—Although deep neural networks (DNN) have achieved state-of-the-art performance in various fields, some unexpected errors are often found in the neural network, which is very dangerous for some tasks requiring high reliability and high security. The non-transparency and unexplainability of Convolutional Neural Networks (CNN) still limit its application in many fields, such as medical care and finance. Despite current studies that have been committed to visualizing the decision process of DNN, most of these methods focus on the low level and do not take into account the prior knowledge of medicine. In this work, we propose an interpretable framework based on key medical concepts, enabling CNN to explain from the perspective of doctors' cognition. We propose an interpretable automatic recognition framework for the ultrasonic standard plane, which uses a concept-based graph convolutional neural network to construct the relationships between key medical concepts, to obtain an interpretation consistent with a doctor's cognition. Extensive experiments have empirically shown that our model can meaningfully explain the decision of the classifier and provide quantitative support.

Index Terms—Ultrasound, Fetus, Computer-aided detection and diagnosis, Graph network models, Geometric deep learning

I. INTRODUCTION

Prenatal ultrasound has become the most commonly used method to detect the anatomical structure of the fetus due to its non-invasive and reproducibility. It also contributes to improving the quality of the population. Reasonable application of Fetal Standard Plane in early obstetric ultrasound examination can play a positive role in the screening and diagnosis of fetal and appendage structural abnormalities. It can detect malformations in the fetal heart, central nervous system, bladder, anterior abdominal wall, limb, and other important tissues and organs early, reduce the birth rate of fetal malformation, and has positive significance for pregnant women, their families, and society. However, in clinical practice, the quality of prenatal ultrasound examination is largely affected by the acquisition techniques and experience of sonographers, which is time-consuming and easy to obtain sections with poor image quality. Therefore, it is particularly important to find a feasible ultrasonic standard plane recognition algorithm.

Prenatal ultrasonography is the most widely used imaging examination for prenatal diagnosis. Detecting a fetal malformation through ultrasonography is a challenging task that requires professional knowledge and extensive experience. Various computer-aided diagnosis methods have been proposed to reduce the burden of ultrasonologist. Since medical decisions may have life-or-death consequences, medical diagnosis applications require not only high performance but also a strong

rationale for judgment[1]. The stakeholders of the medical diagnostic system include doctors, regulatory authorities, and governments. However, to be widely applied to clinical practice, a medical diagnostic system must be trusted by clinicians. In recent years, the explainability technique for Convolutional Neural Networks (CNN) has emerged as an important research topic with substantial progress. Most explainable approaches attempt to explain CNN with saliency [2-7], perturbation-based[8-10], and logical-based[11, 12] methods. However, there are some problems with these explainable methods when applied to clinical practice: (1) They only provide pixel-level explanations of which parts are important to the decision, and do not take into account the interactions between tissues and organs; (2) Sometimes the explanation provided does not necessarily have a causal relationship with the predicted result, and there is a spurious correlation. As Fig. 1. shows, the classifiers judged an input to be a Fetal Femur Standard Plane (FL) based on the discovery of hypoechoic areas rather than the detection of the femur and epiphysis. (3) They don't combine medical knowledge with a doctor's experience.

The rapid development of machine learning, especially deep learning, has revolutionized the way of medical image analysis. Medical artificial intelligence (AI) often needs to solve problems such as image recognition and disease diagnosis, and these problems usually require doctors to accumulate experience and knowledge over a long period. Existing medical AI technologies have achieved good results in disease diagnosis, lesion detection, and segmentation. However, the lack of explainability of deep neural networks restricts its application to practical applications. Compared with other imaging examination methods, such as CT and MRI, ultrasound examination is highly dependent on the experience of ultrasound physicians, which leads to difficulties in the development of AI in the field of ultrasound. Considering that the user of the medical AI is a clinician, our algorithm is interpreted in terms that the clinician can be approved.

Combined with the clinical experience of radiologists, we proposed an interpretable framework based on key medical concepts, enabling CNN to explain from the perspective of doctors' cognition. We use the multi-resolution segmentation method to extract visual concepts, then a prototype network was used to cluster them. Based on prior knowledge provided by clinicals, we further search for the most meaningful concepts for image recognition and use graph convolutional neural networks to model the interaction between these concepts, to simulate the decision-making process of doctors.

In summary, the specific contributions of our work are:

- We combine medical prior knowledge with DNN, which improves the robustness and generalization ability of the model and increases the credibility.
- To improve the accuracy of concept classification, the

morphological and edge information of medical concepts are obtained by differential geometry.

- We use visual concepts that doctors care about and their relative relationships to construct structural diagrams, encode the spatial positions between them, and provide interpretation from the perspective of doctors' cognition.

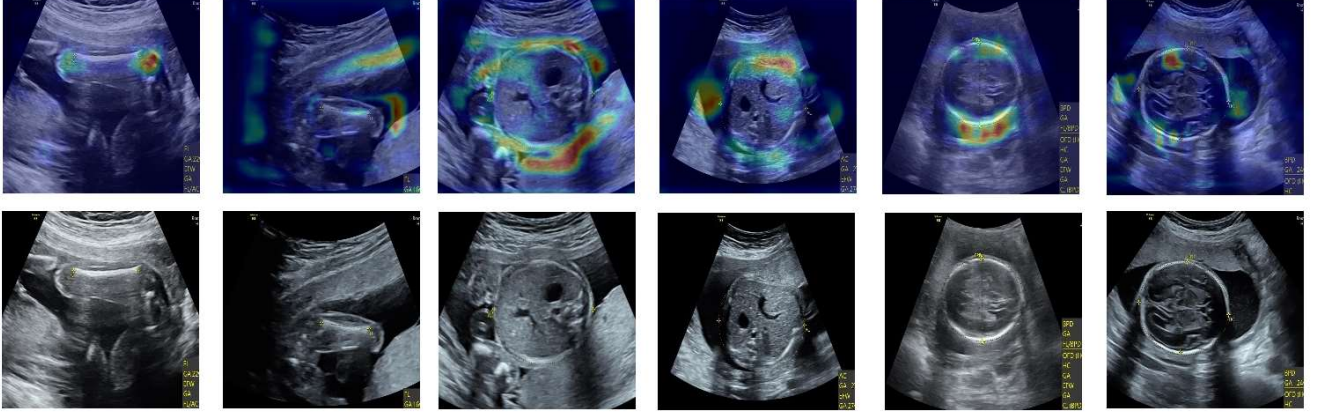


Fig. 1. Failure examples discovered using Grad-CAM for a standard Resnet-50 neural network trained on our fetal ultrasound dataset. In the top row, brighter areas indicate more attention from the neural network. In the bottom row, we show the original images. We can observe that the areas of networks concerned are irrelevant to clinical's decision.

II. RELATED WORK

In this section, we will review the existing literature on interpretable methods, prototype networks, and graph convolutional neural networks.

A. Interpretability in natural images:

The opacity and unexplainability of deep neural networks are the important reasons that restrict its practical application. For medical diagnosis, doctors care more about the reliability and security of AI models than accuracy. Previous works [2],[8],[13-15] have been researched interpretability from many perspectives, including backpropagation-based saliency methods, causal reasoning-based methods, and attribution-based methods.

Backpropagation-based saliency methods generate an attention heatmap to obtain regions that contribute significantly to CNN's decision. One of the earliest studies was to visualize the gradients of neural network layers to obtain the saliency maps, then several researchers made some adjustments to improve the quality of attention heatmaps [16-18]. Other works attempt to combine the gradients and activations, namely feature maps, such as Class Activation Maps (CAM), Grad-CAM, and linear approximation. However, CAM needs to retrain the model, which is computationally expensive. On the other hand, perturbation-based methods find important regions for the classifier by finding the smallest changes to alter the decision of a model. However, these methods are based on pixel-level relations to explain, without modeling human cognition. Elliott et al. [13] present a regularization of adversarial perturbations based upon the perceptual ball (APPB). As semantically meaningful adverse perturbations, it forms a bridge between adversarial perturbations and

counterfactual explanations.

Several recent studies have attempted to extend the interpretability methods to visual concepts that humans intuitively understand. Specifically, Ge et al. [19] proposed a visual reasoning explanation framework based on structural concepts graphs to answer interpretability questions and

potentially provide guidance on improving DNN's performance. Zhang et al. [20] present an explicit visual reasoning method, which incorporates external knowledge and models high-order relational attention.

Our methods also require extracting visual concepts, but it is more adaptable to medical tasks. By combining medical prior knowledge, the meaning of concepts can be more clearly defined and the explanation obtained was more consistent with clinical experience.

B. Other Recommendations Interpretability in medical images

The opacity and unexplainability of deep neural networks are the important reasons that restrict its practical application. For medical diagnosis, doctors care more about the reliability and security of AI models than accuracy. CheXNet[21] localizes pathologies it identifies using CAM, which highlights the areas of the X-ray that are most important for making a particular pathology classification. Based on the assumption that thorax disease usually happens in localized areas and the existence of irregular borders hinders the network performance, a three-branch attention guided convolution neural network (AG-CNN)[22] integrates a global branch to compensate the lost discriminative cues by the local branch. Tang et al [23] attempted to use Guided Grad-CAM and feature occlusion to visualize the feature salience in identifying specific neuropathologies-amyloid plaques and cerebral amyloid angiopathy-in immunohistochemically-stained archival slides.

Although such explanations are medical-friendly, pixel-level regions are neither fit nor meaningful for medical diagnosis. Furthermore, some methods master the ability to automate the human-like diagnostic reasoning process and translate gigapixels directly to a series of interpretable predictions, providing second opinions and encouraging

consensus in clinics[24]. Jaume et al. [14] adopted a biological entity-base graph and yielded intuitive pathological interpretability. They also proposed a set of novel quantitative metrics based on statistics of class separability using pathologically measurable concepts to characterize graph explainers, which relaxes the exhaustive assessment by expert pathologists. Several studies attempt to learn representative features of the disease and make decisions based on these features. Interpretable CNN models are designed to operate in a human-understandable manner [25]. Kim et al. [1] present XProtoNet, which learns representative patterns of each disease from X-ray images and makes a diagnosis on a given X-ray image based on patterns. These works targeted classification tasks in X-ray and pathological images, and there was no attempt to make an interpretable automated diagnosis framework for fetal ultrasound standard plane identification. To this end, we propose an interpretable classification model for the fetal ultrasound standard plane that learns the important structure and location relationship between medical concepts.

C. Graph Neural Networks

Graph convolutional neural network (GCN) [26-28] can process non-Euclidean structured data and model complex information in the graphs, such as heterogeneous connections and high-order connections. In recent years, graph neural networks are often used to learn high-order relationships. For example, Zhao et al.[29] proposed an effective graph-based relation discovery approach to build a contextual understanding of high-order relationships. On the other hand, thanks to its powerful information processing capabilities, GNNs have been widely applied in many visual and linguistic tasks, such as VQA [30-31],[9] image captioning [32-34], and scene understanding tasks[35]. In this study, we use GCN to capture high-order semantic relationships between key medical concepts and provide more credible explanations for clinical.

III. METHOD

In this section, we introduce an interpretable fetal ultrasound standard plane automatic recognition framework based on graph convolutional networks in Fig. 2. The first key idea of our approach is to extract visual concepts approved by clinical in section 3.1, combining with medical prior knowledge. Then, we classify the concepts extracted in 3.1 using prototype networks combined with differential geometry information. Next, we transform the key medical concepts into graph-structured data and introduce a GNN to map the concepts graph to the corresponding class labels in section 3.2. Finally, we explain the decision mechanism of the network and visualize the reasoning process in section 3.3.

A. Equations Medical concepts extractor

Although some interpretation methods based on visual concepts, such as ACE[36] and TACV [37], are very effective in extracting natural images, their performance in medical images is poor. The key step in converting an ultrasound image to graph-structured data is to extract medical concepts from the ultrasound image that are important for differentiation and diagnosis. This ensures that the inputs to our method are medically interpretable and can be directly linked and reasoned

with by the sonographer. Inspired by VRX[19] and XProtoNet [1], we use visual concepts to represent an input image given class-specific knowledge of the pretrained combined medical prior knowledge with visual concept extraction to find the representative features.

First, multi-resolution segmentation methods were applied to extract the superpixels containing the medical concepts. While ACE [36] is reasonably effective in extracting visual concepts in natural images, its performance is poor on ultrasound images. Due to the small foreground area of medical images, most superpixels obtained by multi-resolution methods are backgrounds and irrelevant tissues, which increase the difficulty of concept extraction. As shown in Fig. 4. (bottom), for the Fetal Abdominal Standard Plane (AC), the ACE concepts mostly fall on the areas unrelated to diagnoses, such as tissues and hypoechoic regions. To alleviate this issue, given an image I , we use Grad-CAM[3] to generate attention heatmaps and constrain the target area in the foreground, thereby helping us exclude irrelevant areas to diagnosis.

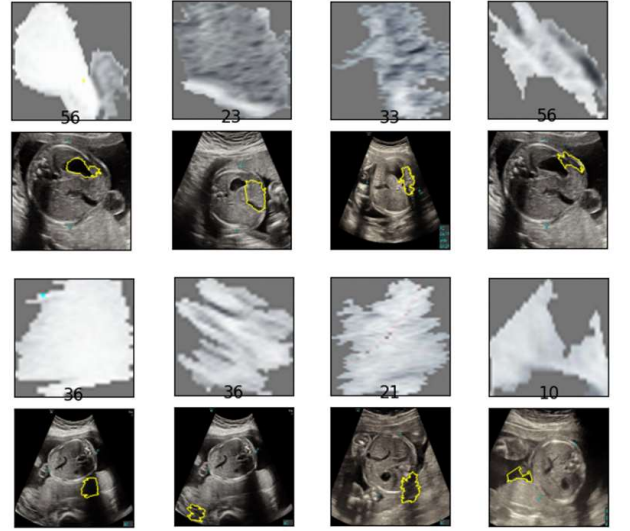


Fig. 3. Concepts discovery with and without medical prior knowledge. The top row uses medical prior knowledge, and the bottom row doesn't use medical prior knowledge.

B. Medical concepts classification based on Prototype Network

The human anatomical structure is consistent among people, and the position and morphological characteristics are similar. Unlike natural images, concepts extracted from medical images have practical significance. Then, two professional sonographers provided prior knowledge of medical concepts, including texture, position, shape, brightness, etc. They also gave us some typical medical concepts examples.

geometric features of concepts. Specifically, we use Jacobian determinant (JD) and curl vectors (CV) as conditional inputs of prototype networks. They play important roles in determining a diffeomorphism, which is an active research topic in differential geometry.

First, we will review the mesh deformation method for generating JD and CV from a given image. We suppose $\Omega_t \subset \mathbb{R}^2$ ($0 \leq t \leq 1$) is a moving domain, $v(x, t)$ is the

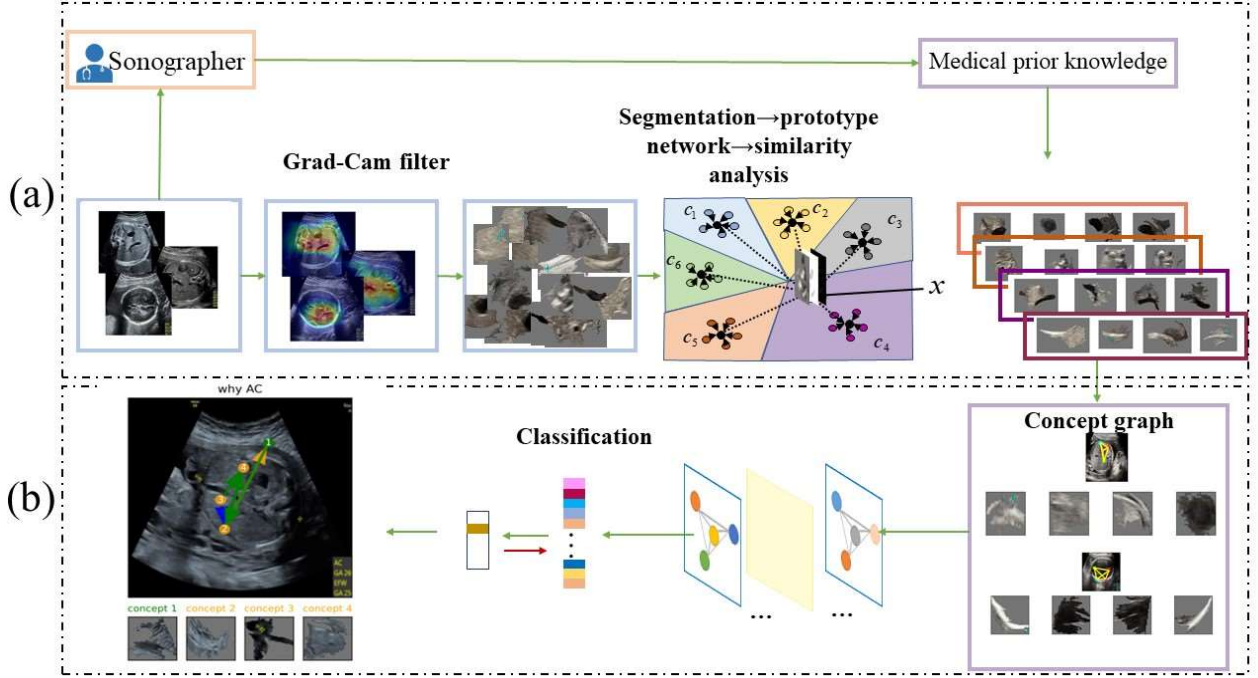


Fig. 2. Pipeline of our proposed framework. (a) extract class-specific medical concepts approved by clinicals, classify them using prototype networks combined with differential geometric information. (b) transform medical concepts to graph-structured data, and use GCN to learn the contribution of nodes (medical concepts) and edges (relationships between concepts) to decision making and to explain the decision-making process of the network.

According to the physician's advice, the visual concept of the Fetal Abdominal Standard Plane can be divided into six classes: low-anechoic liquid, nondiscriminatory soft tissue, gastric vesicles, blood vessels, spine, and a strong echo at the amniotic fluid interface of the abdominal wall (SEA). And the visual concepts from the Fetal Thalamus Standard Plane (HC) also can be divided into six classes: low-anechoic liquid, nondiscriminatory soft tissue, skull, thalamus, third ventricle, and septum pell. Again, the visual concepts from the Fetal Femur Standard Plane can be divided into femurucid, metaphysis, nondiscriminatory soft tissue, and low-anechoic liquid. Therefore, we can find representative medical concepts from concepts generated in 3.1. However, it's time-consuming and laborious to classify extracted concepts for doctors. Inspired by a few-shot learning problem, we use a prototypical network[38] to learn a metric space in which classification can be performed by computing distances to prototype representations of each class. This model can learn a high-dimensional metric space and calculate the distance from the image to the prototype of each class to perform classification.

On the other hand, considering the low resolution of ultrasound images and the influence of inherent speckle noise, we use differential geometry[39] to further extract the

velocity field on $\partial\Omega_t$. In slippery-wall boundary conditions, for any part of $\partial\Omega_t$, we can get $v(x, t) \cdot n = 0$ where n is the outward normal vector of $\partial\Omega_t$. Given a scalar function $f(x, t) > 0 \in C^1(x, t)$ on the domain $\Omega_t \times [0, 1]$, then

$$f(x, 0) = 1 \quad (1)$$

$$\int_{\Omega_t} \frac{1}{f(x, t)} dx = |\Omega_0| \quad (2)$$

A diffeomorphism $\phi(\xi, t): \Omega_0 \rightarrow \Omega_t$ with $\forall t \geq 0$

$$J(\phi(\xi, t)) = \det \nabla \phi(\xi, t) = f(\phi(\xi, t), t) \quad (3)$$

can be created by solving the following differential equations[40]:

$$\begin{cases} \operatorname{div} u(x, t) = -\frac{\partial}{\partial t} \left(\frac{1}{f(x, t)} \right) \\ \operatorname{curl} u(x, t) = 0 \\ u(x, t) = \frac{v(x, t)}{u(x, t)}, \text{ on } \partial\Omega_t \end{cases} \quad (4)$$

$$\begin{cases} \frac{\partial \phi(\xi, t)}{\partial t} = f(\phi(\xi, t), t) u(\phi(\xi, t), t) \\ \phi(\xi, 0) = \xi \end{cases} \quad (5)$$

The deformation method can generate a grid map. Then we can calculate JD and CV based on diffeomorphism. JD represents the size of the grid cell and CV represents the grid cell rotations of grid generation, thus the deformation method can be applied successfully in medical image analysis[40]. The middle and bottom rows of Fig. 4. show the JD and CV of medical concepts from the Fetal Abdominal Standard Plane, and their geometric features further express the difference between concepts. As shown in Fig. 4., we can see that the CV of tissues and liquids are markedly different from other concepts, which further demonstrates the effectiveness of introducing geometric information.

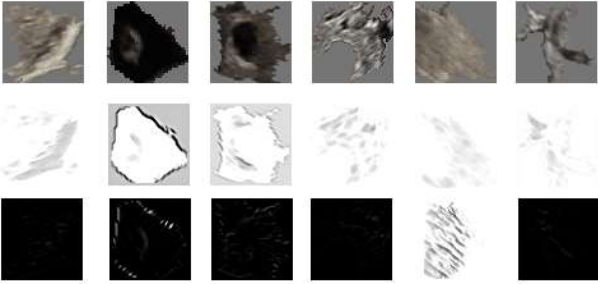


Fig. 4 Generated concepts based on JD and CV. The top row is the original images, the middle row is the images formed by JD, and the bottom row is the images formed by CV. (a), (b), (c), (d), (e), (f) are the SEA, low-anechoic liquid, magenblace, spine, tissue, and vessel from Fetal Abdominal Standard Plane.

C. Concept graph construction

We define a medical concept graph $G := (V, E)$ as a set of nodes V and edges E . $v_i \in V$ denotes a relevant medical concept. The node attributes are the high-order feature encoded by a trained CNN classifier $F(\bullet)$. The properties of directed edges $e_{ij} = (v_i, v_j)$ in the graph have two meanings: 1) The relative relationships of each concept in space, which is initialized by the relative position of two concepts in the image. 2) The correlation between two concepts which were given by

medical prior knowledge. This is essential to the reasoning process of medical concepts.

Based on the above physician-approved medical concepts, we use a trained CNN classifier $F(\bullet)$ to extract the high-order features of medically separable visual concepts and took them as attributes of graph nodes.

Given an input image I , $X \in \mathbb{R}^{C \times H \times W}$ is the feature maps encoded by a trained CNN classifier $F(\bullet)$.

D. Concept graph Learning

Given G , graph-structured data of ultrasound images, we aim to infer the corresponding class of standard section.

We use GraphConv[41] as the backbone of our network. A layer from GCN has two steps: message aggregation and update. Formally, we define a layer as:

$$x_{k+1}^i = W_1 h_k^i + \sum_{j \in N(i)} W_3 C(\alpha_{ji}^c W_2 x_k^j, e_k^{ji}) \quad (6)$$

$$e_{k+1}^{ji} = W_4 e_k^{ji} \quad (7)$$

where x_k^i denotes the features of a node v_i in layer k , W_1 and denotes the shared transformation parameters for the target node v_i and its neighbor node v_j respectively. W_3 and W_4 denote a linear transformation for edge features, $N(i)$ denotes the neighboring nodes of v_i . $C(\bullet)$ denotes concatenation. α_{ji}^c is a predefined prior coefficient, which measures the interdependence between various concepts.

After N iterations, we use an MLP was applied to process graph features and generate an n -dimensional probability distribution vector.

E. Graph decision explainer

As shown in Fig. 2, after an image is fed into our GCN, we can obtain the prediction score $\hat{y} = \Psi(G(x))$. Where Ψ is graph embedding networks and with m layers. Inspired by Grad-CAM, for a specific class c , we obtain its corresponding prediction score \hat{y}^c and calculate the gradients concerning the graph of each layer in GCN as:

$$\omega_i = \frac{\partial \hat{y}^c}{\partial G^i(x_i)} \quad (8)$$

The contribution score of each node (medical concept) or edge to the network's decision is computed as follows:

$$s_i = \omega_i^T G^i(x_i) \quad (9)$$

IV. EXPERIMENTS AND RESULTS

This section describes the analysis of GCN explainability for the classification of fetal standard ultrasound plane. In our experiments, we use VGG19[42] and ResNet[43] as the target neural networks.

A. Implementation details

The data used in this study were all from the Department of Ultrasound, Shenzhen Hospital, Peking University. We collected retrospectively two-dimensional ultrasound data of the brain and abdomen of 860 healthy fetuses from 1070 examined pregnant women using GE Voluson E8 color Doppler ultrasound diagnostic system. The minimum gestational age of the fetus is 16 weeks and the maximum is 39 weeks. And the Fetal Abdominal Standard Plane and Fetal Thalamus Standard Plane in prenatal ultrasound examination were selected for this study. It is clinically prescribed that a standard horizontal section of the fetus can clearly show the lateral fissure, symmetrical thalamus, choroid plexus, septum pellucida, and third ventricle, while the abdominal plane should show the spine, gastric vesicles, liver, and umbilical vein.

B. Training

We conducted our experiments using PyTorch in 11GB NVIDIA GeForce RTX 2080Ti GPU.

In our experiments, we process superpixels by VGG19[42] and ResNet50[43] pre-trained on fetal ultrasound datasets to generate high-level visual attributes of concepts. The GCN architecture for concept-based graph classification is presented in section 3.2. And the GCN classifier was trained for 200 epochs using Adam optimizer, 10^{-1} learning rate, and dynamic adjustment. The best average accuracy of the GCN classifier achieved 92.0%.

C. Qualitative results

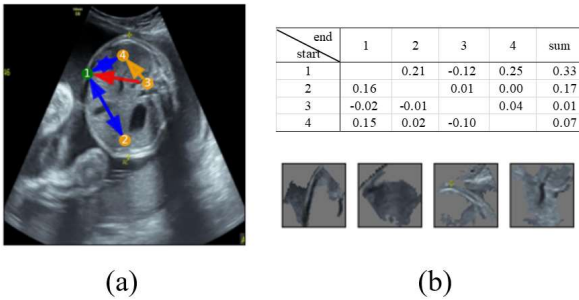


Fig. 5. Quantitative analysis of medical concepts. (a) The important concepts and spatial relationship between them from the fetal abdominal standard plane. (b) The important weights reveal the relationships between concepts, which shows the dependency between medical concepts: concepts 1 and 2 make more contributions than other concepts.

Fig. 6. shows two examples (a correct result and a wrong result) of how our framework help to explain the decision of networks. For the correct prediction, our concept extractor can successfully extract important concepts. As Fig. 6 (a) shows, when the input was correctly predicted as Fetal Abdominal

Standard Plane, the network considers the spine and vessel to be important concepts. From a medical perspective, these extracted concepts are of differential significance to the doctor's diagnosis. On the other hand, from a structural point of view, the edges that connect the nodes also contribute positively to the prediction results, meaning that the discovered concepts have the correct spatial relationships between them. In response to the question of why it's the Fetal Thalamus Standard Plane, most of the concepts detected are bone and cavity of septum pellucidum, which are the unique structure of the brain. From the point of view of the spatial structure, the position of each node is anatomically reasonable. When the network's prediction was wrong, the concepts they found were tissues and liquid, which are not important to diagnosis. This indicates that the prediction is closely related to the discrimination of concepts and our framework can discover areas that have an important impact on a doctor's diagnosis.

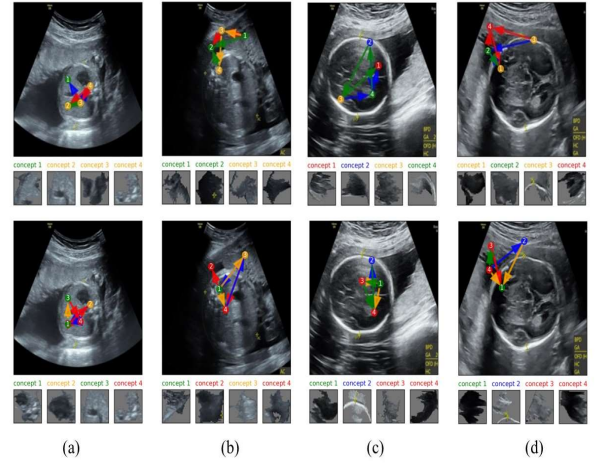


Fig. 6. Medical concept reasoning explanation of Fetal Ultrasound Standard Plane. The top row is the prediction result based on ResNet50, and the bottom row is the prediction result based on VGG19 (a) correct prediction of Fetal Abdominal Standard Plane. (b) wrong prediction of Fetal Abdominal Standard Plane prediction. (c) correct prediction of Fetal Thalamus Standard Plane. (d) wrong prediction of Fetal Thalamus Standard Plane.

Based on the above explanation, MGE can reasonably explain the logic of the decision mechanism in the network from the perspective of high-order relations and discover the reasons for the failure of the decision.

D. Prediction analysis based on extracted concepts

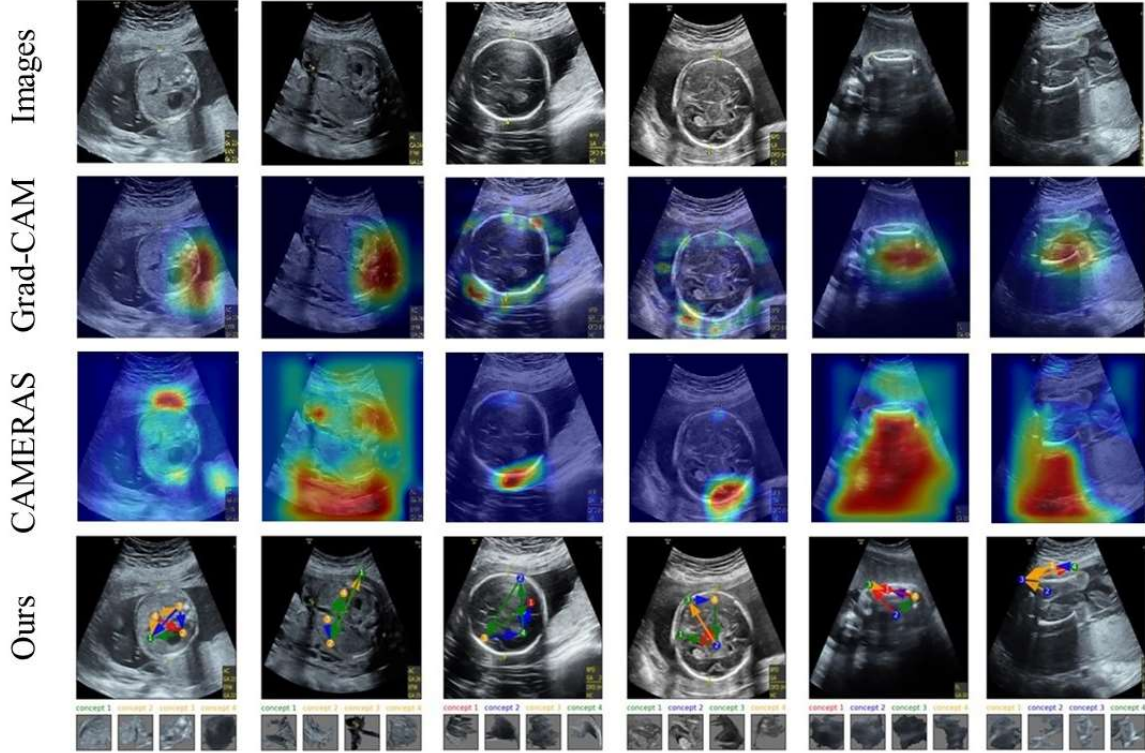
Due to the complexity and diversity of medical images, even professional physicians may make mistakes in diagnosis. Therefore, we believe that medical AI also has a capability upper limit. We cannot make our model have 100% accuracy in practical application, in fact, due to the diversity of data, all models cannot achieve this ideal goal. However, we expect our model to have a reasonable assessment of its own ability to reject difficult samples rather than give a false result.

Our framework not only can provide classification results, but also quantitative scores for concepts and structure. Based on the importance weights of concepts and structure, we can evaluate the results with confidence. Sonographers often do not make decisions based on a single concept when classifying Fetal Ultrasound Standard Plane. Therefore, based on this experience, we can further evaluate the network. When three of the four concept scores of the network are negative, we consider the prediction results of the network to be unreliable. After excluding unreliable results, we reevaluated the classification performance of the network, and the results are shown in Table

Table 2. Comparison of model accuracy of VGG19 before and after screening.

accuracy	original	selected
AC	0.906	0.968
FL	0.944	0.956
HC	0.909	0.924
average	0.920	0.949

E. Evaluation from clinical



1. It can be found that the classification accuracy of the network is significantly improved after screening according to the

To evaluate the effectiveness of extracted medical concepts, we conduct user studies with 5 professional

Fig. 7. Comparison of explainability methods on Fetal Standard Planes based on ResNet50.

importance score of the concept.

Table 1. Comparison of model accuracy of ResNet50 before and after screening.

accuracy	original	selected
AC	0.903	0.968
FL	0.922	0.957
HC	0.832	0.870
average	0.886	0.923

sonographers. Participants were required to have at least five years of clinical experience.

We explain the classification results of VGG19 and ResNet50, and compare them with other interpretation methods. We randomly selected 100 images and interpretation results from each class and showed them to doctors. For visualization of ResNet50, participants were shown four sections: original image, interpretation results of Grad-CAM, CAMERAS and our framework. For visualization of VGG19, participants were shown five sections: original image, interpretation results of Grad-CAM, CAMERAS, Adversarial Perturbations and our framework. Fig. 7. and Fig. 8. are examples of explainability methods on Fetal Standard Planes. We asked participants to imagine facing the following situations:

We will conduct reliability analysis for classification models (VGG19 and ResNet50) trained on Fetal Standard Planes. We asked you to imagine that you are part of the team that will test this in clinical and wants to understand when the model is

unreliable and perform operations upon failures. All participants were shown results from VGG19 and ResNet50. They agreed that the introduction of interpretable results would enhance the trust of users in the classification model. However, in contrast to many other approaches that highlight important regions, our methods construct the higher-order semantic relationships between concepts and it has obvious advantages in identifying errors. And all five doctors in the study agreed that our method was more clinically useful.

great use in computer-aided diagnosis and contribute to the promotion and application of medical AI.

ACKNOWLEDGMENT

This research was supported by Foundation of Shenzhen Science and Technology Planning Project (NO. GJHZ2020 0731095205015) and the International Cooperation Foundation of Tsinghua Shenzhen International Graduate School (No.

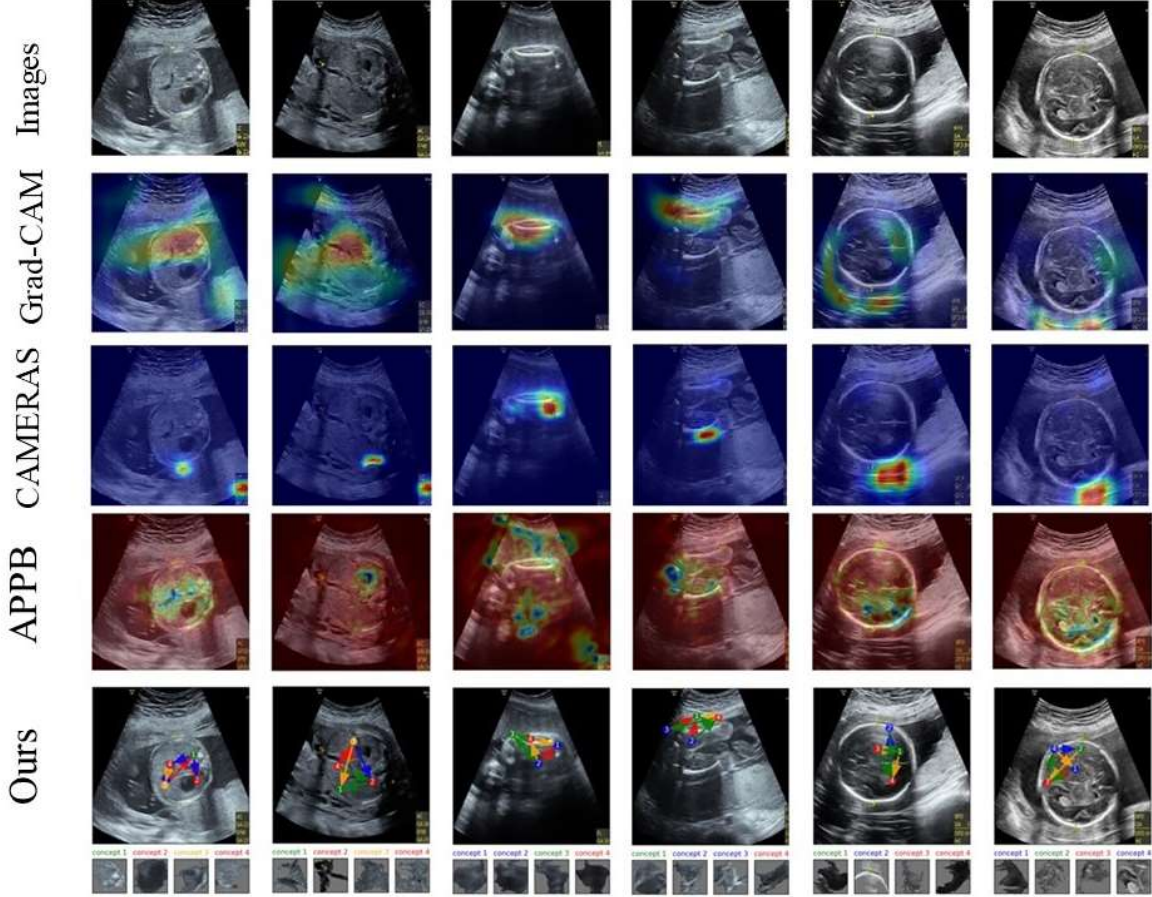


Fig. 8. Comparison of explainability methods on Fetal Standard Planes based on VGG19.

HW2021001).

V. CONCLUSION

In this work, we proposed an approach to interpreting the decision mechanism of a neural network from the perspective of human cognition. We present a medical reasoning explanation framework combining medical prior knowledge and differential geometry information which can extract effective medical concepts for diagnosis and model the spatial relationship between them. The experiments in section 4 showed that our framework can visualize the reasoning process of the neural network at the conceptual level that clinicians can understand, which is more likely to be approved by clinicians. Furthermore, with the interpretation from MGE, we demonstrate that it can provide confidence for prediction and error analysis. The proposed explainable method contains terms in the medical field, which is consistent with the knowledge and experience of clinicians. We believe that it can potentially be of

REFERENCES

- [1] E. Kim, S. Kim, M. Seo, and S. Yoon, "XProtoNet: Diagnosis in Chest Radiography with Global and Local Explanations," in Proceedings of the IEEE/CVF Conference on Computer Vision and Pattern Recognition, 2021, pp. 15719-15728.
- [2] B. Zhou, A. Khosla, A. Lapedriza, A. Oliva, A. Torralba, and Ieee, "Learning Deep Features for Discriminative Localization," in 2016 IEEE Conference on Computer Vision and Pattern Recognition (CVPR), Seattle, WA, 2016, pp. 2921-2929, 2016.
- [3] R. R. Selvaraju, M. Cogswell, A. Das, R. Vedantam, D. Parikh, and D. Batra, "Grad-CAM: Visual Explanations from Deep Networks via Gradient-Based Localization," International Journal of Computer Vision, vol. 128, no. 2, pp. 336-359, Feb 2020.
- [4] S. A. Rebuffi, R. Fong, J. Xu, and A. Vedaldi, "There and back again: revisiting backpropagation saliency methods (2020 IEEE/CVF Conference on Computer Vision and Pattern Recognition). 2020, pp. 8836-45.
- [5] M. A. K. Jalwana, N. Akhtar, M. Bennamoun, and A. Mian, CAMERAS: Enhanced Resolution And Sanity preserving Class Activation

Mapping for image saliency (2021 IEEE/CVF Conference on Computer Vision and Pattern Recognition). 2021, pp. 16322-16331.

[6] J. R. Lee, S. Kim, I. Park, T. Eo, and D. Hwang, "Relevance-CAM: Your Model Already Knows Where To Look," in Proceedings of the IEEE/CVF Conference on Computer Vision and Pattern Recognition, 2021, pp. 14944-14953.

[7] K. Simonyan, A. Vedaldi, and A. J. a. p. a. Zisserman, "Deep inside convolutional networks: Visualising image classification models and saliency maps," 2013.

[8] V. Petsiuk et al., "Black-box explanation of object detectors via saliency maps," in Proceedings of the IEEE/CVF Conference on Computer Vision and Pattern Recognition, 2021, pp. 11443-11452.

[9] S. Jiaxin, Z. Hanwang, and L. Juanzi, Explainable and explicit visual reasoning over scene graphs (2019 IEEE/CVF Conference on Computer Vision and Pattern Recognition). 2019, pp. 8368-76.

[10] M. Sundararajan, A. Taly, and Q. Yan, "Axiomatic Attribution for Deep Networks," 2017.

[11] S. Alaniz, D. Marcos, B. Schiele, and Z. Akata, "Learning Decision Trees Recurrently Through Communication," in Proceedings of the IEEE/CVF Conference on Computer Vision and Pattern Recognition, 2021, pp. 13518-13527.

[12] M. Nauta, R. van Bree, and C. Seifert, "Neural Prototype Trees for Interpretable Fine-grained Image Recognition," in Proceedings of the IEEE/CVF Conference on Computer Vision and Pattern Recognition, 2021, pp. 14933-14943.

[13] A. Elliott, S. Law, and C. Russell, "Explaining Classifiers using Adversarial Perturbations on the Perceptual Ball," in Proceedings of the IEEE/CVF Conference on Computer Vision and Pattern Recognition, 2021, pp. 10693-10702.

[14] G. Jaume et al., "Quantifying explainers of graph neural networks in computational pathology," in Proceedings of the IEEE/CVF Conference on Computer Vision and Pattern Recognition, 2021, pp. 8106-8116.

[15] Q. Zhang, Y. Yang, H. Ma, and Y. N. Wu, "Interpreting CNNs via Decision Trees," 2018.

[16] M. D. Zeiler and R. Fergus, "Visualizing and understanding convolutional networks," in European conference on computer vision, 2014, pp. 818-833: Springer.

[17] J. T. Springenberg, A. Dosovitskiy, T. Brox, and M. J. a. p. a. Riedmiller, "Striving for simplicity: The all convolutional net," 2014.

[18] D. Smilkov, N. Thorat, B. Kim, F. Viégas, and M. J. a. p. a. Wattenberg, "Smoothgrad: removing noise by adding noise," 2017.

[19] Y. Ge et al., "A Peek Into the Reasoning of Neural Networks: Interpreting with Structural Visual Concepts," in Proceedings of the IEEE/CVF Conference on Computer Vision and Pattern Recognition, 2021, pp. 2195-2204.

[20] Y. Zhang, M. Jiang, and Q. Zhao, "Explicit Knowledge Incorporation for Visual Reasoning," in Proceedings of the IEEE/CVF Conference on Computer Vision and Pattern Recognition, 2021, pp. 1356-1365.

[21] P. Rajpurkar et al., "CheXnet: Radiologist-level pneumonia detection on chest x-rays with deep learning," 2017.

[22] Q. Guan, Y. Huang, Z. Zhong, Z. Zheng, L. Zheng, and Y. Yang, "Diagnose like a Radiologist: Attention Guided Convolutional Neural Network for Thorax Disease Classification," 2018.

[23] Z. Tang, K. V. Chuang, C. Decarli, L. W. Jin, and B. N. Dugger, "Interpretable classification of Alzheimer's disease pathologies with a convolutional neural network pipeline," 2018.

[24] Z. Zhang et al., "Pathologist-level interpretable whole-slide cancer diagnosis with deep learning," vol. 1, no. 5, pp. 236-245, 2019.

[25] C. J. N. M. I. Rudin, "Stop explaining black box machine learning models for high stakes decisions and use interpretable models instead," vol. 1, no. 5, pp. 206-215, 2019.

[26] W.-L. Chiang et al., "Cluster-GCN: An Efficient Algorithm for Training Deep and Large Graph Convolutional Networks," in 25th ACM SIGKDD International Conference on Knowledge Discovery & Data Mining (KDD), Anchorage, AK, 2019, pp. 257-266, 2019.

[27] M. Schlichtkrull, T. N. Kipf, P. Bloem, R. Van Den Berg, I. Titov, and M. Welling, "Modeling Relational Data with Graph Convolutional Networks arXiv," arXiv, pp. 10 pp.-10 pp., 17 March 2017.

[28] X. Yue et al., "Graph embedding on biomedical networks: methods, applications and evaluations," (in English), Bioinformatics, Article vol. 36, no. 4, pp. 1241-1251, Feb 2020.

[29] Y. Zhao, K. Yan, F. Huang, and J. Li, "Graph-Based High-Order Relation Discovery for Fine-Grained Recognition," in Proceedings of the IEEE/CVF Conference on Computer Vision and Pattern Recognition, 2021, pp. 15079-15088.

[30] S. Ghosh, G. Burachas, A. Ray, and A. Ziskind, "Generating Natural Language Explanations for Visual Question Answering using Scene Graphs and Visual Attention arXiv," arXiv, pp. 7 pp.-7 pp., 15 Feb. 2019.

[31] D. Teney, L. Lingqiao, and A. Van DenHengel, "Graph-structured representations for visual question answering arXiv," arXiv, pp. 9 pp.-9 pp., suppl. 7 pp., 19 2016.

[32] J. Gu et al., "Unpaired Image Captioning via Scene Graph Alignments," in IEEE/CVF International Conference on Computer Vision (ICCV), Seoul, SOUTH KOREA, 2019, pp. 10322-10331, 2019.

[33] N. Xu, A.-A. Liu, J. Liu, W. Nie, and Y. Su, "Scene graph captioner: Image captioning based on structural visual representation," Journal of Visual Communication and Image Representation, vol. 58, pp. 477-485, Jan 2019.

[34] Y. Xu, T. Kaihua, Z. Hanwang, and C. Jianfei, Auto-Encoding Scene Graphs for Image Captioning (2019 IEEE/CVF Conference on Computer Vision and Pattern Recognition). 2019, pp. 10677-86.

[35] Y. Li, W. Ouyang, B. Zhou, K. Wang, X. Wang, and Ieee, "Scene Graph Generation from Objects, Phrases and Region Captions," in 16th IEEE International Conference on Computer Vision (ICCV), Venice, ITALY, 2017, pp. 1270-1279, 2017.

[36] A. Ghorbani, J. Wexler, J. Zou, and B. Kim, "Towards Automatic Concept-based Explanations," in 33rd Conference on Neural Information Processing Systems (NeurIPS), Vancouver, CANADA, 2019, vol. 32, 2019.

[37] B. Kim et al., "Interpretability Beyond Feature Attribution: Quantitative Testing with Concept Activation Vectors (TCAV)," in 35th International Conference on Machine Learning (ICML), Stockholm, SWEDEN, 2018, vol. 80, 2018.

[38] J. Wang and Y. Zhai, "Prototypical Siamese Networks for Few-shot Learning," in 10th IEEE International Conference on Electronics Information and Emergency Communication (IEEE ICEIEC), Electr Network, 2020, pp. 178-181, 2020.

[39] Y. Zhu, Z. Zhou, G. Liao, K. Yuan, and Ieee, "CSRGAN: MEDICAL IMAGE SUPER-RESOLUTION USING A GENERATIVE ADVERSARIAL NETWORK," in 17th IEEE International Symposium on Biomedical Imaging Workshops (IEEE ISBI), Iowa City, IA, 2020, 2020.

[40] X. X. Cai, B. Jiang, G. J. C. Liao, and M. w. Applications, "Adaptive grid generation based on the least-squares finite-element method," vol. 48, no. 7-8, pp. 1077-1085, 2004.

[41] C. Morris et al., "Weisfeiler and leman go neural: Higher-order graph neural networks," in Proceedings of the AAAI Conference on Artificial Intelligence, 2019, vol. 33, no. 01, pp. 4602-4609.

[42] K. Simonyan and A. J. a. p. a. Zisserman, "Very deep convolutional networks for large-scale image recognition," 2014.

[43] K. He, X. Zhang, S. Ren, and J. Sun, "Deep residual learning for image recognition," in Proceedings of the IEEE conference on computer vision and pattern recognition, 2016, pp. 770-778.